TOXICOLOGY AND APPLIED PHARMACOLOGY **140,** 471–486 (1996)
ARTICLE NO. 0244

A Physiologically Based Pharmacokinetic Model for Arsenic Exposure

II. Validation and Application in Humans

SABINE MANN,* PIERRE-OLIVIER DROZ,* AND MARIE VAHTER†

**Institute of Occupational Health Sciences, Lausanne University, Lausanne, Switzerland; and †Institute of Environmental Medicine, Karolinska Institutet, Stockholm, Sweden*

Received November 29, 1995; accepted May 21, 1996

A Physiologically Based Pharmacokinetic Model for Arsenic Exposure. II. Validation and Application in Humans. MANN, S., DROZ, P.-O., AND VAHTER, M. (1996). *Toxicol. Appl. Pharmacol.* **140, 471–486.**

A physiologically based pharmacokinetic model (PB-PK) for inorganic arsenic exposure in humans has been developed. This model is an extension of a PB-PK model for hamsters and rabbits, with adjustments for body weight, metabolic rates, and absorption rates. It describes the absorption, distribution, metabolism, and excretion of arsenate, arsenite (As(III)), methyl arsonate, and dimethyl arsinate, the four major metabolites of inorganic arsenic. The routes of intake considered are inhalation of arsenic dust and fumes and oral intake of arsenic via drinking water and food. The PB-PK model for the oral exposure route is validated using data on urinary excretion after repeated oral exposure to As(III) as well as after exposure to inorganic As via drinking water. Absorption by inhalation is validated using data on urinary excretion after occupational exposure to arsenic trioxide dust and fumes. In both cases, the model gives satisfactory results for urinary excretion of the four As metabolites. The PB-PK model is also used in the description of the effects on the kinetics of exposure via different routes and for the simulation of various realistic exposure scenarios.

The use of physiologically based pharmacokinetic models (PB-PK) to describe the pharmacokinetic behavior of organic compounds is now well known and mastered. These models are often used in risk assessment because they allow the introduction of biological concepts. So far, PB-PK models have been developed mainly for solvents. In general, they are based on two types of data: (i) animal-specific parameters, such as tissue and blood volumes and blood perfusion; and (ii) chemical-compound-related parameters, such as solubility or partition coefficients of the solvents in the various tissues and in blood, and metabolic clearance and excretion rates (Andersen, 1991). For solvents, the tissue–gas partition coefficients can be either measured or estimated using water and oil air partition coefficients (Droz, 1978; Fiserova-Bergerova, 1983).

For metals and metaloids such as arsenic, much less is known concerning pharmacokinetic modeling. A major difference from organic compounds is that there is no evidence that metals diffuse freely and rapidly over the entire walls of the capillaries and alveolar membranes. Another problem is related to the assessment of the affinity constants of the metals for the different tissues.

In the present work, a PB-PK model for the kinetics of arsenic metabolites in humans after oral and inhalation exposure to inorganic arsenic is presented. This model is an extension of an animal model previously developed for hamsters and rabbits (Mann *et al.,* 1996). The objective of the present work is to integrate different aspects of the present knowledge on arsenic pharmacokinetics in order to compare urinary excretion at different doses after inhalation exposure to (As(V)) with inhalation exposure to arsenite (As(III)) and oral exposure to As(V) in humans.

METHOD

A list of symbols used in this paper is given in the Appendix.

Description of the physiologically based pharmacokinetic model. The model consists of six tissue compartments, four absorption compartments, and three excretion compartments (Fig. 1). The six tissue compartments—blood, liver, kidneys, lungs, skin, and other tissues (other)—were chosen according to the affinity of arsenic for the tissues. The ''other'' compartment represents the remaining tissues, including bones and muscles. Blood constitutes one compartment with two subcompartments in equilibrium: plasma and red blood cells (RBCs). Only arsenic metabolites present in the plasma subcompartment are considered available for distribution to the tissues, because arsenic in the RBCs is bound and therefore considered unavailable for exchange with tissues.

Two routes of absorption are considered in the model (Fig. 1): oral intake for simulation of exposure via drinking water and food and inhalation exposure for simulation of occupational or community exposure to arsenic-containing aerosols. The oral exposure route includes absorption from the gastrointestinal (GI) tract, which is considered a transit compartment. The dose of arsenic ingested is diluted in the stomach contents and then made available for absorption in the GI tract. This approach is different from that

0041-008X/96 $18.00

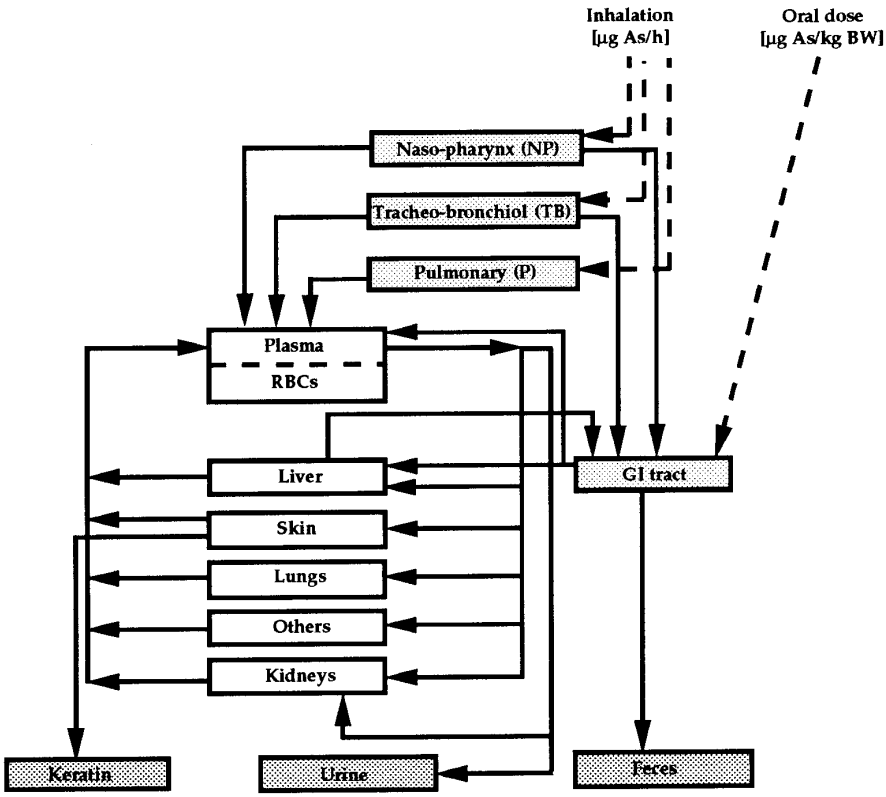

FIG. 1. Schematic presentation of the PB-PK model showing the exposure routes, the tissues *i*, and the excretion routes for one arsenic metabolite. This diagram is repeated four times in the model, once for each arsenic metabolite.

described in the model for animals (Mann *et al.*, 1996). It was introduced to facilitate scaling between species (including some physiological parameters of the GI tract; see Eqs. (20)–(27) in the Appendix). The absorption of arsenic from the GI tract to the liver is described using first-order kinetics. The inhalation exposure route includes three transit compartments: the nasopharynx (NP), the tracheobronchial (TB), and the pulmonary (P) (ACGIH, 1993). The absorption from these compartments into the plasma is described using first-order kinetics, which itself is a function of the surface area of the compartment. The deposition and clearance of dust particles in the lungs are described below.

The distribution of arsenic to the tissues depends on their blood perfusion, the permeability of the capillary membranes, and the affinity of the tissues for the arsenic metabolites. In the PB-PK model, these parameters are scaled according to body weight (Lindstedt, 1992; Fiserova-Bergerova and Hughes, 1983) in order to make the model applicable to different animal species. The physiological data, obtained after scaling and used in the model for humans, are given in Table 1. The scaling parameters are presented in a previous publication (Mann *et al.*, 1996).

Arsenic distribution to the tissues is described using a diffusion-limited model. For membrane transfer, nonionized compounds diffuse freely through the capillary membranes, whereas ionized compounds diffuse only through the pores of the membranes (Berner and Cooper, 1985). This transfer is described in more detail in a previous publication (Mann *et al.*, 1996).

The affinity of arsenic metabolites for the different tissues is assumed to be independent of the concentration and of the animal species (rabbit, hamster, and human) at the exposure levels considered. The tissue affinity constant K represents the affinity of the arsenic metabolites for the tissues, with no specification of the tissue compounds with which it might bind. The K values (Table 2) have been obtained by fitting the model to experimental data for hamsters and rabbits (Mann *et al.*, 1996). For RBCs, K values obtained *in vitro* were used (Mann *et al.*, 1995).

The biotransformation of arsenic in the body consists of an oxidation/reduction and two methylation reactions. The oxidation/reduction of inorganic arsenic takes place in the plasma (Marafante *et al.*, 1985), but the reduction can also occur intracellularly, e.g., in the kidneys (Ginsburg, 1965). Based on several studies showing that the methylation of As(III) takes place mainly in the liver cytosol by enzymatic catalysis (Vahter and Marafante, 1988; Buchet and Lauwerys, 1987, 1988), the model describes the two methylation steps as occurring in the liver only, according to Michaelis–Menten (M–M) reactions (V_m is the M–M maximum rate constant and K_m is the M–M constant).

Lung model: Aerosol penetration, deposition, and clearance. In general, inhalation of polydispersed aerosols is described using three lung compartments: NP, TB, and P regions (ISO, 1991). In the model, the deposition of the aerosol in the three respiratory regions is dependent on the breathing frequency, tidal volume, particle size distribution, and concentration of the dust. Such a description allows the simulation of exposure to aerosols of different particle size distributions in situations with different physical work loads.

The deposition in the lungs is calculated in two steps based on a log-normal distribution of the aerosol: (i) penetration into the three compartments and (ii) deposition of the penetrated aerosol fraction. The penetration in the three compartments is calculated using the equations proposed by Soderholm (1989). The calculation of the deposition in the upper part of the respiratory tract (NP) is based on the model of the ICPR task group (James *et al.*, 1989). The deposition of the aerosol in the two lower compart-

TABLE 1
Physiological Data Used in the Model for Humans

Physiological parameter	Organ	Units	Human (body weight = 70 kg)
Blood volume		ml	5,222
Organ weight	Liver	g	1,856
	Kidneys	g	314
	Lungs	g	584
	Skin	g	6,225
	Others	g	55,277
Lumen volume	Stomach	ml	274
	Small intestine	ml	393
Blood flow	Cardiac output	Liters/min	5.29
	Liver, hepatic	Liters/min	0.32
	Liver, splanchic	Liters/min	1.02
	Kidneys	Liters/min	0.95
	Lungs	Liters/min	0.16
	Skin	Liters/min	0.35
	Others	Liters/min	2.49
Creatinine	Male	g/day	1.7
Creatinine	Female	g/day	1.0
Clearance	GFR	ml/min	156
Small intestine length		cm	481
Nasopharynx area		cm^2	177
Tracheobronchial area		cm^2	5,036
Pulmonary area		cm^2	712,471
Total capillary surface area		cm^2	1.877×10^6

ments of the lungs (TB and P) is calculated using the equation of Taulbee and Yu (1975) and the lung ''Model A'' of Weibel (1963). The deposited fraction of the airborne concentration for a given aerodynamic diameter for the three pulmonary compartments (NP, TB, and P) is equal to the fraction of the aerosol penetrating times the fraction of penetrating aerosol that is deposited. The details of the mathematical equations of the model are given in the Appendix.

The results of the predicted dust depositions in the lungs are shown in Fig. 2. The aerosol deposition was calculated for particles with diameters $\geqslant 0.1$ μm. For industrial aerosols, with a typical mass median aerodynamic diameter (MMAD) of 5.0 μm and a geometric standard deviation (GSD) of 2.1, particles with aerodynamic diameters $\leqslant 0.1$ μm can be neglected. For aerosols of very low MMAD, the deposition of small particles should be introduced into the model.

TABLE 2
Tissue Affinity Constants Obtained by Fitting the Model for Rabbits and Hamsters and Used for Humans

Tissue *i*	K_i, AsV	K_i, AsIII	K_i, MMA	K_i, DMA
Liver	1	200	10	1
Kidneys	40	20	100	5
Lungs	1	1	1	20
Skin	1	60	50	1
RBCs	0.2	1.5	0.2	0.2
Others	10	40	1	1

Note. Data from Mann *et al.* (1996).

Lung clearance occurs via two different mechanisms: (i) clearance by solubilization and absorption from all three compartments into the plasma and (ii) mechanical clearance. For mechanical clearance from the nasopharynx and the tracheobronchial compartments to the GI tract, first-order rate constants were taken from the literature (Johnson and Milencoff, 1989). The rate constant for the alveolar mechanical lung clearance from the pulmonary compartment to the tracheobronchial compartment was taken from Guilmette and Mewhinney (1989). For arsenic, no data on the absorption rate constant are available in the literature. In the PB-PK model, the absorption rate constant per unit of surface area is assumed to depend on the solubility

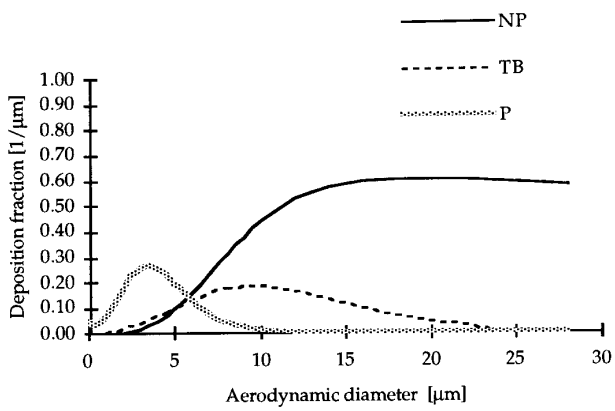

FIG. 2. Dust deposition in the three lung compartments used in the PB-PK model (physical work load, light activity; tidal volume, 1200 ml; breathing frequency, 16 min^{-1}).

of the aerosol and assumed to be the same in all three compartments. This unit absorption rate was obtained by fitting the model to experimental data.

Data obtained by fitting. When physiological parameters were not available and calculations could not be based on physicochemical properties, missing values were obtained by fitting. This was done by simulation of the experimental scenarios, while varying the unknown constants and visually comparing the simulated results with experimental data. For the present model, the unknown parameters that had to be fitted were the GI tract absorption rates, the lung absorption rates, and the metabolic rate constants. A body weight of 70 kg was assumed for all simulations.

Various experimental data were used for adjustment of the metabolic rate constants: various oxidation states of the inorganic arsenic and various exposure doses. To determine the ratio V_m/K_m, a low-dose exposure was first chosen, and then the V_m was adjusted with a high-dose exposure. The metabolic rate constants were adjusted using experimental data on urinary excretion of arsenic following a single oral dose of As(III) (Buchet *et al.*, 1981a) or As(V) in volunteers (Tam *et al.*, 1979). The total arsenic excretion in urine in experimental data was used to fit the GI tract absorption rate constants of As(III), As(V), monomethyl arsonate (MMA), and dimethyl arsinate (DMA). Oral exposures to MMA and DMA were included in the development of the model to validate their distribution and excretion.

The lung absorption rate constant was obtained by fitting the total urinary excretion of arsenic as predicted with the model to experimental data from occupational exposure to arsenic trioxide (Offergelt *et al.*, 1992).

Validation. The human PB-PK model was validated using data from studies of repeated oral intake of sodium meta-arsenite in volunteers (Buchet *et al.*, 1981b), occupational exposure to arsenic trioxide and elemental arsenic (Vahter *et al.*, 1986), and community exposure to As(V) via drinking water (Harrington *et al.*, 1978; Valentine *et al.*, 1979).

Applications. Risk assessment is often based on the results of epidemiological studies involving exposure from different sources, e.g., inhalation exposure and oral intake. For this purpose it would be useful to have information on the differences in the tissue concentrations and urinary excretions in relation to the route of exposure. Similarly, it is essential to investigate the effect of the oxidation state of the absorbed inorganic arsenic. To compare data from different exposure studies and to evaluate possible differences between some current arsenic recommended exposure limits, realistic scenarios representing community and occupational exposure were also simulated.

RESULTS

Development of the PB-PK Model for Humans

The first two sets of experimental data were used to estimate by fitting the metabolic rates in humans and the GI tract absorption rates. The first set of experimental data used in the fitting of the PB-PK model concerns oral exposure of volunteers to a single dose of arsenic acid (^{74}As) (Tam *et al.*, 1979). In this study, six male volunteers were administered 0.01 μg As (6 μCi) following overnight fasting. The results predicted by the model for the cumulative urinary excretions of the As metabolites are compared with the experimental data (mean of six males volunteers) in Fig. 3. The percentage of dose excreted in urine for the first 5 days following the exposure was 57.9 $\pm$ 1.5% in the experimental study, whereas the model predicts 50.0%. There is a good agreement between the predicted results and the experimental data for the urinary excretion of all As metabolites.

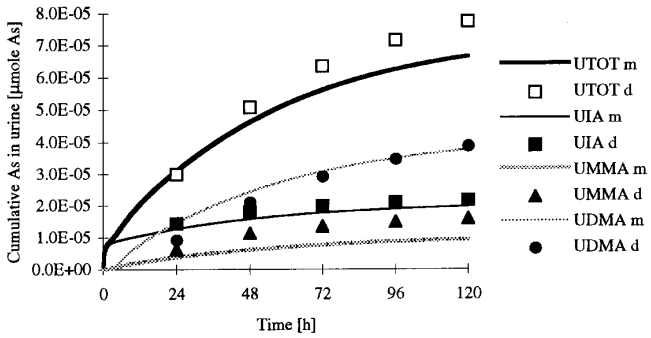

FIG. 3. Comparison of predicted urinary excretion of As metabolites following a single oral intake of arsenic acid with experimental data from six male volunteers (Tam *et al.*, 1979). The graph represents the cumulative urinary excretions of the As metabolites (m, model; d, experimental data).

The second set of experimental data used for fitting the PB-PK model was obtained from Buchet *et al.* (1981a). In this study, human volunteers ingested a single oral dose (500 μg As) of $NaAsO_2$, MMA, or DMA. A comparison of the predicted cumulative urinary excretion of arsenic metabolites with the experimental data is shown in Fig. 4. The simulation results correlate well with the experimental data for the three different arsenic compounds.

The first-order rate constant for the absorption of arsenic trioxide from the lungs to the plasma was estimated by fitting to experimental data from occupational exposure (Offergelt *et al.*, 1992). In this study, the exposure to airborne arsenic and the urinary excretion of inorganic arsenic and methylated metabolites of 18 workers were followed over a 1-week period. The personal daily airborne arsenic values were used for the simulation. The predicted urinary excretion for 1 worker, chosen as representative of the group, is shown in Fig. 5. It shows a good correlation between the model and the experimental data for urinary excretion of total arsenic and the As metabolites. Figure 6 summarizes the results obtained for all 18 workers for 1 week; urinary excretions of As metabolites (both experimental and predicted by the model) are plotted as a function of the airborne arsenic concentration. The purpose of this figure is to show the contribution of occupational variability to urinary excretion variability.

The fitted GI tract and lung absorption rate constants are given in Table 3. The fitted metabolic rate constants are presented in Table 4.

Validation in Humans

The first validation was carried out using data from an experimental study on repeated oral intake of $NaAsO_2$ (four different dose levels) in four volunteers (one volunteer per dose level) once a day for 5 consecutive days (Buchet *et al.*, 1981b). For the simulation, a body weight of 70 kg was

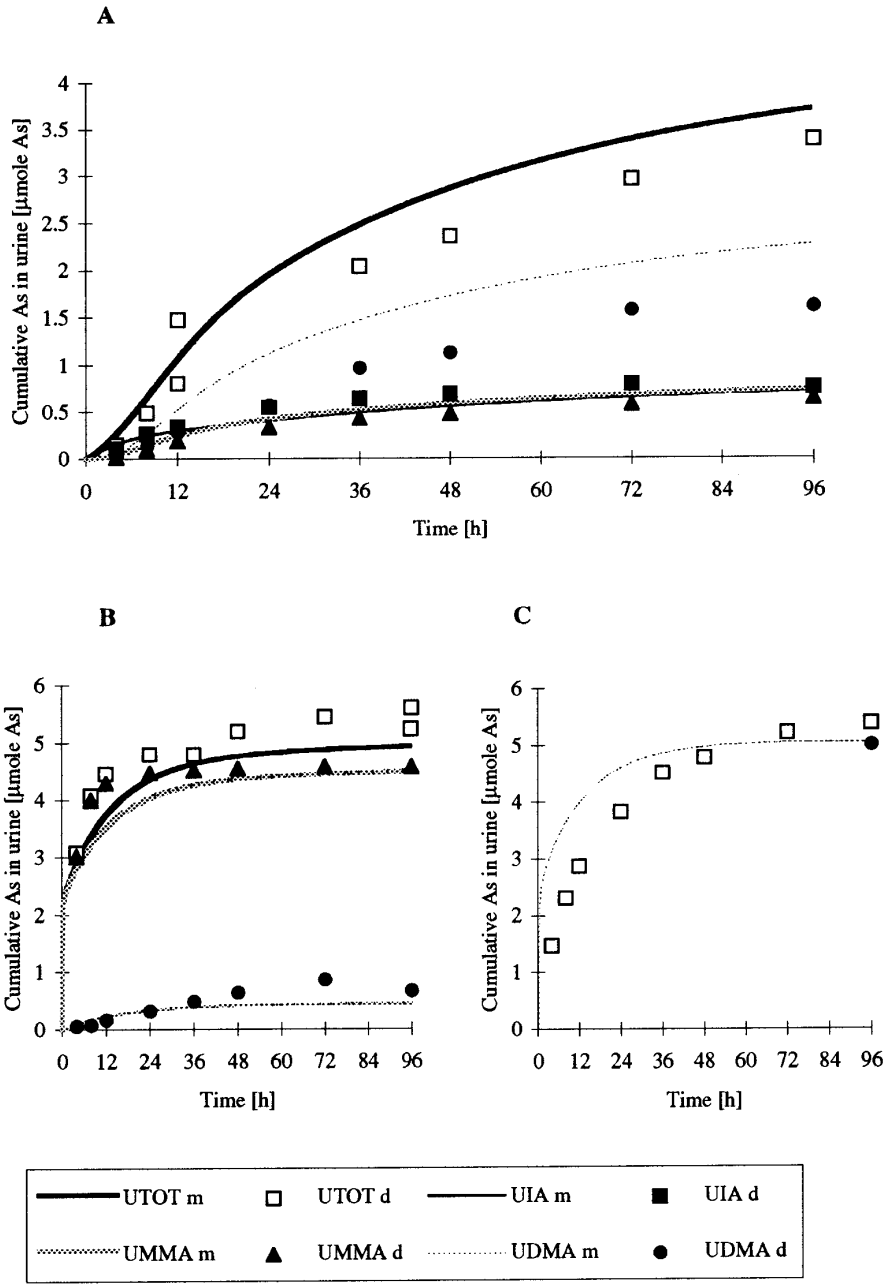

FIG. 4. Comparison of predicted urinary excretion of As metabolites following a single oral intake of 500 μg As with experimental data from Buchet *et al.* (1981a). The three graphs represent the cumulative urinary excretions of the As metabolites following exposure to (A) $NaAsO_2$, (B) MMA, and (C) DMA (m, model; d, experimental data).

assumed. The results of the cumulative urinary excretions of As metabolites at the lowest and highest doses are shown in Fig. 7. Small differences in the excretions of the As metabolites in urine can be noted. However, because the experimental data involved only one person per dose level, the differences might be explained by interindividual variation.

For validation of oral exposure to arsenic via drinking water, the simulations were performed assuming a daily exposure to As(V) evenly distributed over 15 hr per day (7 AM to 10 PM), 7 days a week for a person of 70 kg body weight. The excretion data obtained (reference man) were then compared with the average total As excretion in a population group (Harrington *et al.*, 1978; Valentine *et al.*, 1979). For the second study, the upper and lower ranges in the

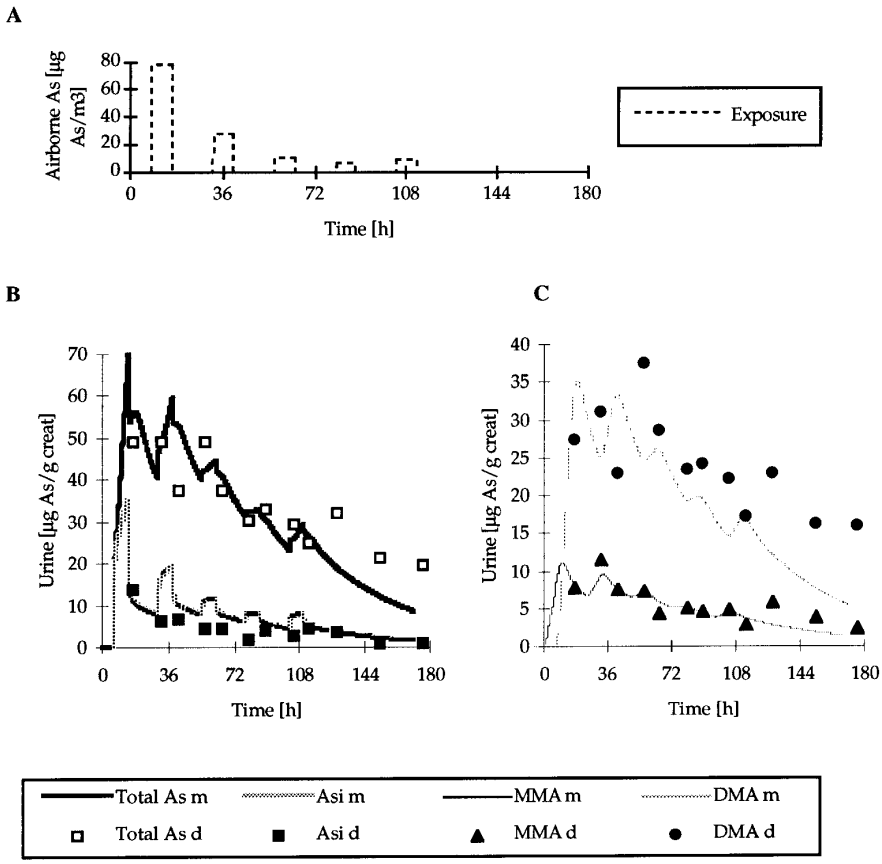

FIG. 5. Comparison of predicted urinary excretion of As metabolites following occupational exposure to airborne arsenic with experimental data from one representative subject in a group of 18 studied (Offergelt *et al.,* 1992). (A) The measured As airborne exposure during the working week. (B and C) The comparison between the model and the experimental data for urinary excretion of As metabolites.

population were also considered. The results of the validation of the model with drinking water indicate a fairly good overall agreement, especially with the report by Harrington *et al.* (1978) (Table 5). However, it must be noted that the comparison is based on the daily excretion for a reference man (70 kg) and the average excretion in a population. There are also some uncertainties concerning the estimation of the daily dose for the population. The results show, however, that the absorption rate of As(V) used in the model is in agreement with the absorption of As from drinking water.

The model for inhalation of As(III) was validated using occupational exposure data reported by Vahter *et al.* (1986). The experimental data included the airborne arsenic concentration for 2 working days and the corresponding urinary arsenic concentrations of six workers. Workers B and C were exposed in an arsenic metal plant, worker D–F were exposed in an arsenic trioxide refinery, and worker A was a female assistant (not previously exposed to arsenic) who supervised the sampling at the arsenic metal plant. Except for subject A, the exposure during the previous week was considered in the simulation (the same Monday morning urine concentration for the results of the model as measured experimentally). In Fig. 8, the simulated 2-day industrial exposure and the urinary excretion of total As are compared with the experimental data for six workers.

Applications

Route of exposure and oxidation state. Three simulations were carried out with the model: oral exposure to As(III), inhalation of As(III), and oral exposure to As(V). Both oral and inhalation exposures are assumed to occur 7 days per week, at a dose of 100 μg As/day. In the case of oral exposure, the simulation involves continuous intake of arsenic for 15 hr per day (from 7 AM to 10 PM). In the case of inhalation exposure, occupational exposure for 8 hr per day, from 8 AM to 4 PM, is assumed. A daily dose of 100 μg As/day would correspond to 8 hr of occupational exposure to an airborne As concentration of 27 μg As/m^3 assuming a tidal volume of 1.2 liters, a breathing frequency of 16 min^{-1}, a MMAD of 5.0 μg, and a GSD of 2.1 (ICPR, 1992).

Figure 9 presents a comparison of the relative distribution

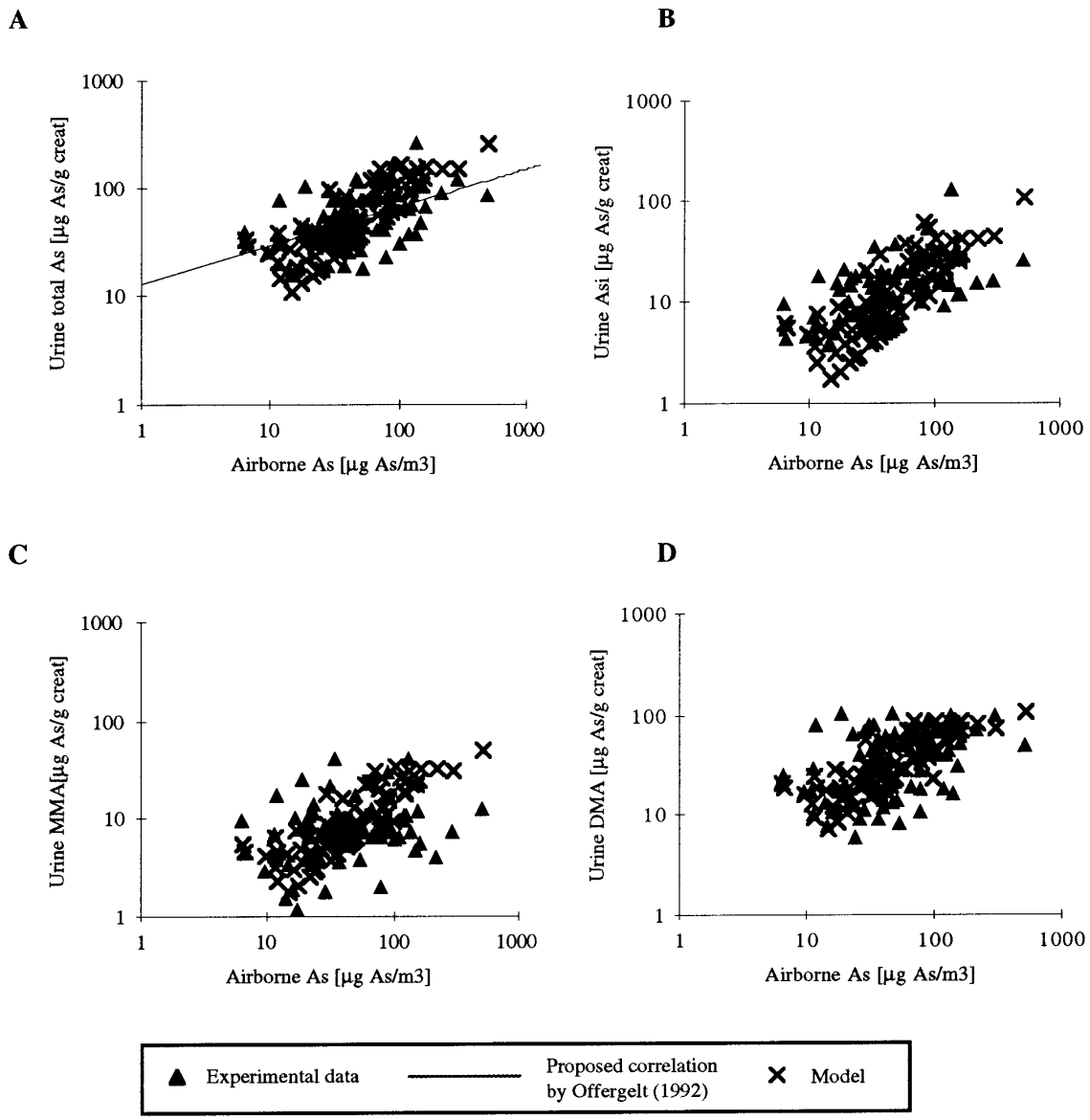

FIG. 6. Comparison of PB-PK model with data from a study of occupational exposure to As_2O_3 (Offergelt *et al.*, 1992) showing the correlation between the arsenic metabolites in postshift urine and the concentrations of airborne arsenic. The four graphs represent the arsenic metabolites in the postshift urine of 18 workers: (A) total As, (B) inorganic As, (C) MMA, and (D) DMA.

of the predicted As metabolites in urine, in the morning and in the evening, for the three scenarios. The predicted arsenic metabolite distributions in the morning and evening urine are summarized in Table 6 and compared with the data reported in a number of exposure studies reviewed by Hopenhayn-Rich *et al.* (1993).

An important issue raised in risk assessment is the linearity of the dose–response curve. To address this point, single oral doses of As(III) and As(V) at different concentrations were simulated. The predicted cumulative As metabolite excretions in urine during the first 24 hr after exposure to As(III) and As(V) are presented in Fig. 10.

Application to realistic exposure scenarios. Simulation of the urinary excretion of As following exposure to drinking water (As(V)) containing 10 μg As/liter (WHO, 1993) or 50 μg As/liter (current drinking water U.S. standard) was carried out. The exposures were simulated for a person weighing 70 kg and drinking 2 liters of water per day (assumed to be continuous for 15 hr from 7 AM to 10 PM), 7 days per week. Urinary As excretion following exposure via drinking water was compared to that following inhalation exposure in an industrial environment (arsenic trioxide refinery, As(III)). The latter was simulated for a person of 70 kg, with exposure occurring for 8 hr per day (8 AM–4 PM),

TABLE 3
Fitted GI Tract and Lung Absorption Rate Constants for Arsenic Compounds in Humans

Exposure As compound	GI tract absorption rate constant (hr^{-1})	Lung absorption unit rate constant[a] ($cm^{-2} \cdot hr^{-1}$)
AsV		
Arsenic acid	2.5	—
Drinking water	2.5	—
AsIII		
$NaAsO_2$	1.8	—
As_2O_3 dust	—	0.01
MMA	5.1	—
DMA	4.4	—

[a] First-order rate constant for absorption per unit of lung compartment surface area.

5 days a week. The airborne arsenic concentration used was 10 μg As/m^3 (ACGIH, 1993) with an aerosol of MMAD of 5.0 μm and a GSD of 2.1. Breathing parameters were 1.2 liters tidal volume and 16 min^{-1} breathing frequency (ICPR, 1992).

The results of the total As urinary excretion for the three exposure scenarios are shown in Fig. 11. The increase in total urinary excretion of arsenic after exposure to drinking water containing 10 μg As/liter reaches a steady state between 6 and 9 μg As/g creatinine. This level of arsenic concentration in urine is in the same range as the background level for urinary arsenic, which was not included in the model. After exposure to drinking water containing 50 μg As/liter, the urinary concentration of total As is between 32 and 43 μg As/g creatinine. During occupational exposure to airborne arsenic at a concentration of 10 $\mu g/m^3$, the urinary excretion increases from Monday to Friday from 7 to 25 μg As/g creatinine. The urinary concentration on Sunday is in the same range as the urinary excretion after exposure to drinking water containing 10 μg As/liter.

TABLE 4
Fitted Metabolic Rate Constants for Arsenic in Humans

Oxidation/reduction	First order
Reduction	1.37 hr^{-1}
Oxidation	1.83 hr^{-1}
Kidney reduction	1.75 hr^{-1}
Methylation	Michaelis–Menten
1st step	$K_{m_{MMA}}$ 0.15 μmol/liter
	$V_{m_{MMA}}$ 0.4 μmol/liter/hr
2nd step	$K_{m_{DMA}}$ 0.15 μmol/liter
	$V_{m_{DMA}}$ 0.5 μmol/liter/hr

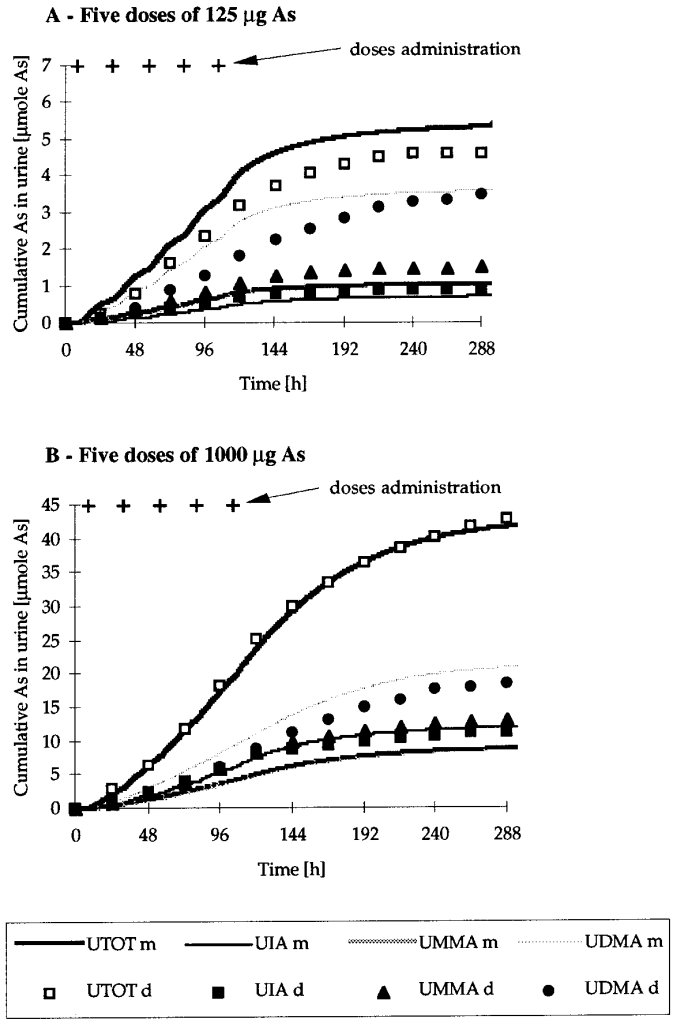

FIG. 7. Validation of the model with data from repeated oral intake of $NaAsO_2$ in one human volunteer (for 5 days, once a day; Buchet *et al.*, 1981b). The graphs represent the cumulative urinary excretion of the As metabolites at a dose of (A) 125 As and (B) 1000 μg As (m, model; d, experimental data).

DISCUSSION

A PB-PK model previously developed for hamsters and rabbits (Mann *et al.*, 1996) has now been extrapolated to humans. In the process, absorption and metabolic rate constants had to be adjusted to take species differences into account. All other parameters remained the same or were scaled according to body weight. The results of urinary excretion of arsenic metabolites obtained with the model are in good agreement with experimental data obtained in studies in which people have been exposed to arsenic orally (intake by volunteers and population exposure) or by inhalation (workers). However, in some cases discrepancies exist. For example, the urinary excretion of DMA after oral intake of

TABLE 5
Validation of the Model for Drinking Water Exposure to As(V)

Daily dose (2 liters/day) (μg As/day)	Urinary total As excretion (μg As/g creatinine)				
	PB-PK model average	Population experimental data			
		Minimum	Average	Maximum	Reference[a]
786	295.3	6.0	134.8	543.5	A
246	93.1	3.3	41.5	90.1	A
197	74.4	6.4	47.2	133.6	A
103	38.8	6.5	37.0	165.2	A
<12	4.5	1.8	6.4	22.6	A
324	122.6	—	146.8	—	B
106	40.0	—	37.2	—	B
80	30.4	—	35.5	—	B
38	14.2	—	32.3	—	B
19	7.2	—	31.5	—	B

[a] Population survey data from (A) Valentine *et al.* (1979) and (B) Harrington *et al.* (1978).

$NaAsO_2$ seems to be overestimated by the model in some cases (Buchet *et al.*, 1981a; Fig. 4A) but agrees well with other data (Tam *et al.*, 1979; Fig. 3). The reason for this is not clear. Individual differences cannot be excluded as an explanation because the two groups consisted of few subjects. Theoretically, it could be an indication of inaccurate description of nonlinearity in the model, mainly with regard to metabolism. Mechanisms other than saturation of the enzymatic system could be present and should be tested to describe the different doses of the two studies. To elucidate the metabolism further, more studies at different doses would be needed.

Some differences in DMA excretion in urine were also found during simulation of repeated ingestion of arsenic, as indicated in Fig. 7. In this case, agreement is satisfactory at high doses but not at low doses during the first 2 days of exposure. During the first hours after oral exposure to DMA, the predicted excretion of DMA in urine seems to be too high (Fig. 4C). This tends to show that the DMA excretion rate in urine, which is made equal to the glomerular filtration rate in the model, is too high. This can also be seen for occupational exposure, when DMA excretion in urine decreases too rapidly during the weekend (Fig. 5).

The comparisons of predicted urinary As excretion for occupational exposure with experimental data among As-exposed workers shown in Figs. 5 and 6 are also satisfactory, taking into account the limited field studies available. Figure 6 provides some interesting information concerning interindividual variability. It is often thought that variability in biological samples observed under field conditions is derived exclusively from differences in metabolism and distribution between individuals. Figure 6 shows that the model can simulate a similar range of variability, only based on exposure fluctuations. Individual differences in arsenic excretion are therefore not the sole determinant of variability in biological monitoring results; variability may even be a minor component. Because the model does not take into account any individual variability in metabolism and exposure (work load and breathing parameters), the variability observed with the model is due only to previous exposure. For example, the evening urine reflects not only the exposure during the shift but also the exposure of the previous days. This is translated as a corresponding variability in the exposure–excretion relationships.

The model for occupational exposure was validated with experimental data from Vahter *et al.* (1986). In Fig. 8, some discrepancies can be observed, mainly for workers D–F. The first two workers are described as wearing respirators during the second day of observation. The elevated results measured in urine could be a result of inefficient respiratory protection. It may also reflect, as suggested in the paper, other routes of intake, especially oral intake of arsenic due to poor personal hygiene (Vahter *et al.*, 1986).

The results of predicted As metabolite excretion in urine after repeated exposure for 2 weeks further confirm the results of the model (Table 6) and give interesting information on the distribution of the As metabolites in urine (Fig. 9). The model results indicate that a significant amount of As(V) is found in the urine only after absorption of As(V). In the case of exposure to As(III), the fraction of As(V) in urine is close to zero. More striking is the fact that the fraction of As(V) in urine is much higher in the evening urine samples than in the morning samples (morning, 2% As(V); evening, 10% As(V)), probably due to the intake of As(V) during the day. Thus, it is important to standardize the urine sampling time before any firm conclusions about the As(III)/

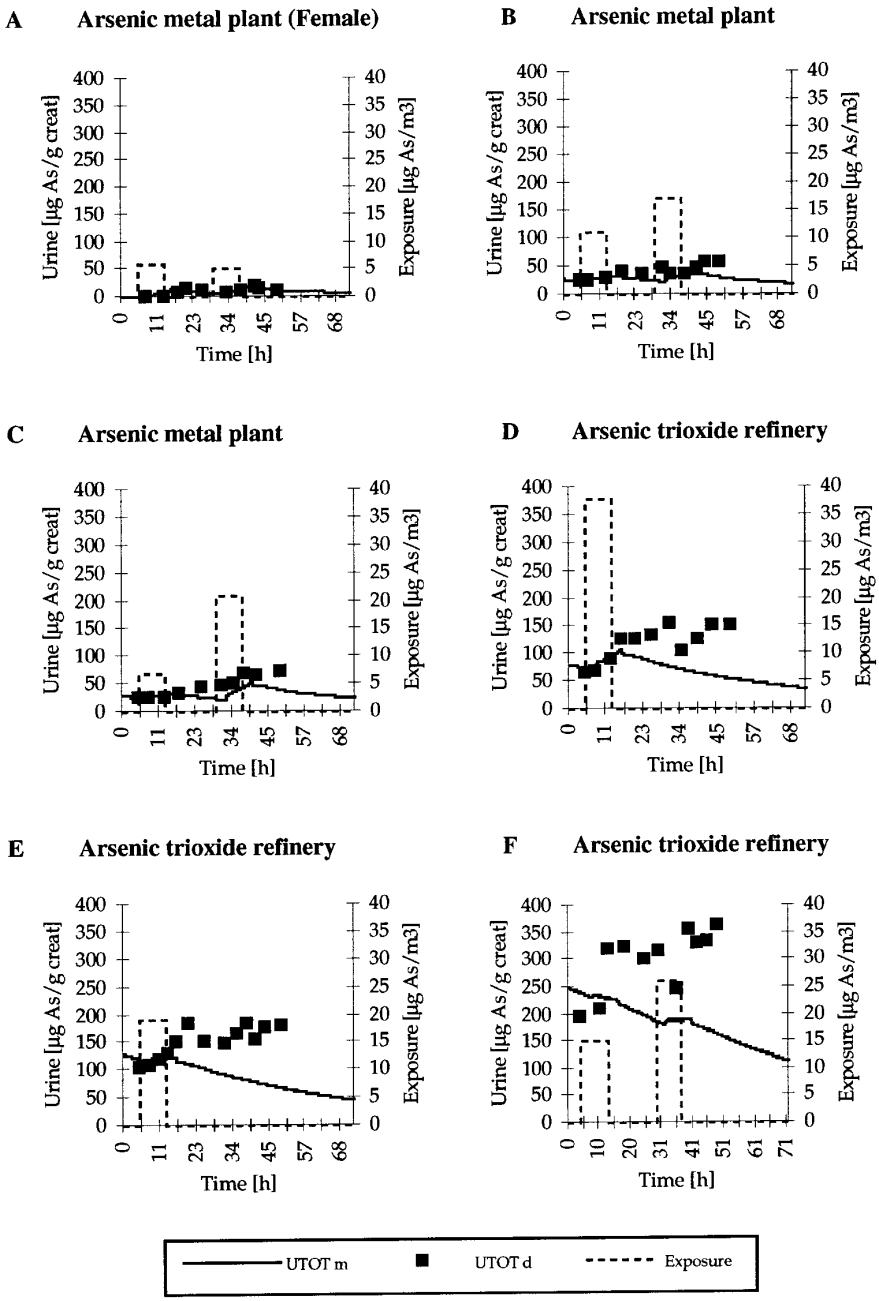

FIG. 8. Validation of the model with data from a study of occupational exposure to arsenic trioxide and elemental arsenic (Vahter *et al.*, 1986). The graphs represent the urinary excretion of total arsenic (m, model; d, experimental data) and the airborne As level during the workshift (dotted line). Subjects A–C were exposed in a arsenic metal plant and subjects D–F were exposed in an arsenic trioxide refinery.

As(V) distribution pattern can be drawn. Figure 9 also shows that the total concentration of arsenic metabolites in the urine varies with the exposure route and the chemical form of arsenic absorbed (at the same dose level). The predicted urinary excretion of arsenic was higher for the inhalation of As(III) than for the ingestion of As(III).

The question of nonlinearity in arsenic metabolism is of great interest in the risk assessment process when effects observed at high doses are to be extrapolated to lower doses. It seems clear that in animals given very high doses of As (between 2 and 5 mg As/kg body wt) there is nonlinearity in the methylation of arsenic (Vahter, 1981; Hughes *et al.*, 1994). However, the results of a number of studies on the pattern of urinary As metabolites following environmental,

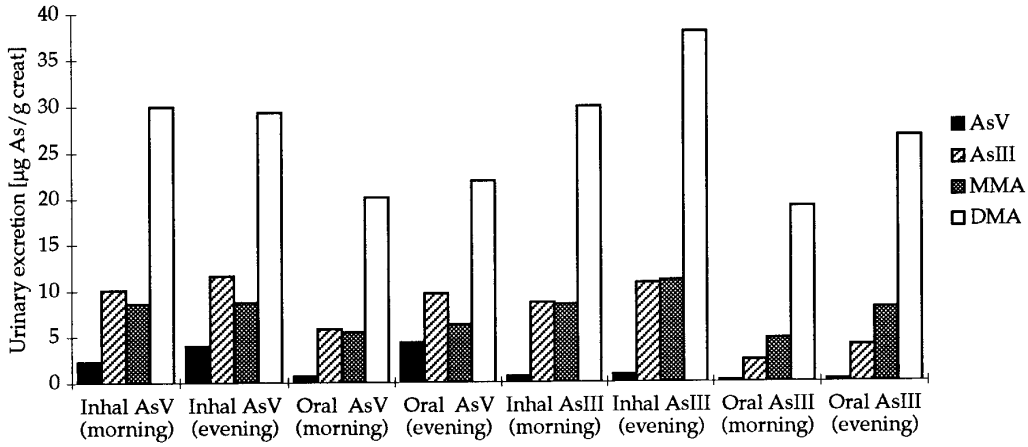

FIG. 9. Comparison of urinary excretions results obtained with the model after 3 weeks of exposure to As(III) or As(V) with two intake routes, oral and inhalation (100 μg As/day, 7 days/week).

experimental, or occupational exposure do not indicate a saturation of the methylation of inorganic arsenic (Hopenhayn-Rich *et al.*, 1993). In the range of exposure levels studied with the PB-PK model (highest dose, 15 μg As/kg body wt), the predicted results show a decrease in the methylation capacity that can be observed with a decline of DMA proportion in urine (Fig. 10). This furthermore seems to apply mainly to As(III) exposures. Probably after As(V) exposure, the time needed for its reduction to As(III) reduces the maximum concentration of As(III) in the liver and therefore reduces the saturation or inhibition of the two methylation steps. The predicted increase in excretion of inorganic arsenic in urine as a function of dose indicates saturation of the first methylation step. On the other hand, MMA remains relatively unchanged in the same range, indicating concomitant saturation of the second methylation step.

One major objective of the present model is to compare the urinary excretion of As metabolites under different exposure conditions, especially different routes of absorption and different oxidation states of the absorbed inorganic arsenic. The results predicted with the model (Fig. 11) indicate that consumption of drinking water containing 50 μg As/liter leads to higher urinary arsenic excretion than occupational exposure to 10 μg/m^3 (ACGIH, 1993). Considering that the target populations are different and that in the case of exposure via drinking water, the entire population, including children, elderly, and people with various diseases, must be protected, this should be studied further. The predicted urinary excretion after exposure at a dose level of the recommended drinking water standard for arsenic by WHO is lower than that after occupational exposure to 10 μg As/m^3.

At this stage, the PB-PK model can be used mainly to compare urinary excretion of arsenic metabolites after oral or inhalation exposure. The constants estimated within the

TABLE 6
Predicted Arsenic Metabolite Distribution in Urine after Daily Exposure As(V) or As(III) for 3 Weeks

			As metabolite distribution in urine (%)		
	Exposure	Time of urine collection	As_i	MMA	DMA
Results predicted with the PB-PK model	Oral AsV	Morning	20	17	63
	Oral AsV	Evening	33	15	52
	Oral AsIII	Morning	10	18	72
	Oral AsIII	Evening	11	21	69
	Inhalation AsIII	Morning	19	18	63
	Inhalation AsIII	Evening	19	18	63
Observed in human studies (Hopenhayn-Rich, 1993)		Background exposure	12–38 (mean = 21)	4–32 (mean = 15)	32–78 (mean = 65)
		Occupational and environmental exposure	12–27 (mean = 20)	9–22 (mean = 15)	60–70 (mean = 65)

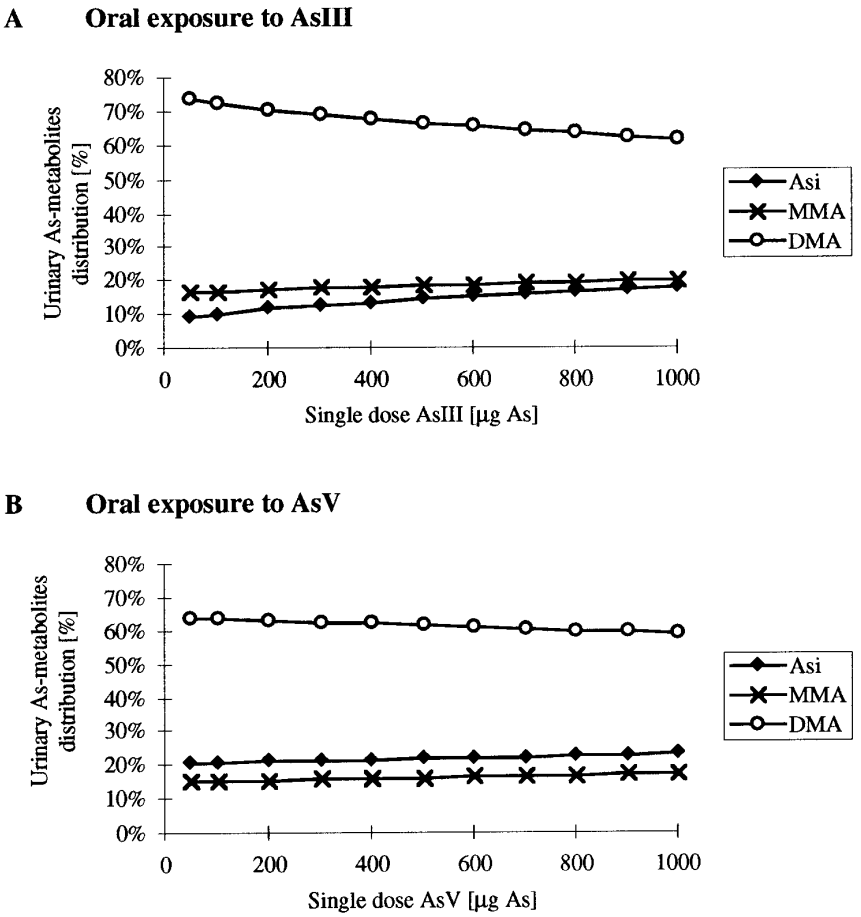

FIG. 10. Predicted cumulative As metabolite distribution in urine 24 hr after a single oral dose of As(III) (A) and As(V) (B).

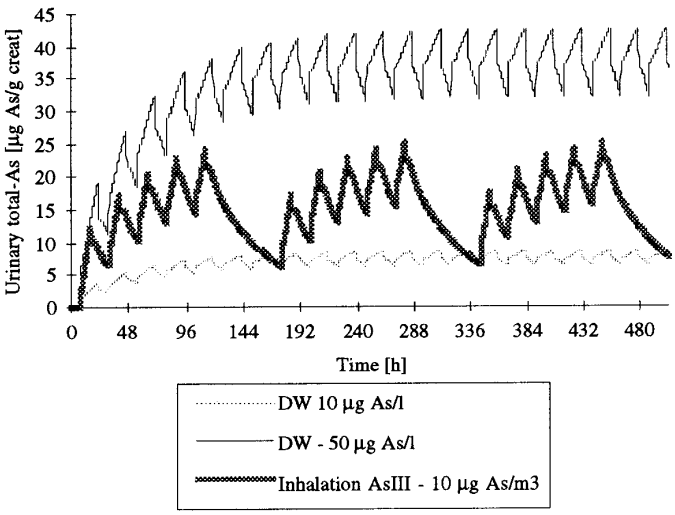

FIG. 11. Comparison of urinary total As excretion results obtained with the model for three realistic scenarios; (a) drinking water exposure, 10 μg As/liter, 2 liters/day; (b) drinking water exposure, 50 μg As/liter, 2 liters/day; and (c) copper smelter exposure, 10 μg As/m^3.

model should not be used separately, due to the large number of estimated parameters. Great uncertainties concerning their physiological values remain.

The PB-PK model could also be used to compare the metabolism and excretion of arsenic after inhalation of aerosols containing As(V). This requires, however, knowledge of the absorption rates of As(V) chemicals and some experimental data to validate the model. This will be carried out in future work when experimental data become available.

APPENDIX

List of Symbols

Symbol	Definition	Unit
a	Scaling equation constant	—
A	Cross-sectional area of one tube in a lung generation	cm^2
$\hat{a}$	Volume occuppied by alveoli in a given generation	cm^3
b	Scaling equation power constant	—
BF	Breathing frequency	min^{-1}

BW	Body weight	kg
CONC	Air concentration	μg As/m^3
D	Deposited fraction	—
Dae	Aerodynamic diameter	μm
D_B	Particle Brownian diffusion	cm^2/sec
DMA	Dimethyl arsinate	—
DW	Drinking water	—
g	Gravity constant	m/sec
GI	Gastrointestinal	—
GFR	Glomerular filtration rate	ml/min
GSD	Geometric standard deviation	—
k	Boltzmann's constant	J/K
K	Tissue affinity constant	—
K_m	Michaelis–Menten constant	μmol As
$K_{m_{DMA}}$	Second methylation Michaelis–Menten constant	μmol As
$K_{m_{MMA}}$	First methylation Michaelis–Menten constant	μmol As
k_{ox}	Oxidation first-order rate constant	hr^{-1}
k_{red}	Reduction first-order rate constant	hr^{-1}
MMA	Monomethyl arsonate	—
MMAD	Mass median aerodynamic diameter	μm
NP	Nasopharynx	—
N_{alv}	Total number of alveoli in the lung	—
P	Pulmonary	—
Q	Blood flow	ml/hr
RBCs	Red blood cells	—
S	Fraction of aerosol particles deposit	sec^{-1}
SG	Fraction of dust deposit in one generation	—
SI	Inhalable dust fraction	—
SNP	Fraction of the dust in the NP that deposits	—
SPP	Fraction of the dust in the P that deposits	—
SR	Respirable dust fraction	—
ST	Thoracic dust fraction	—
STB	Fraction of the dust in the TB that deposits	—
T	Absolute temperature	K
t	Time for an aerosol front to reach a given alveoli in the lung	sec
TB	Tracheobronchial	—
TCS	Total capillary surface	cm^2
TV	Tidal volume	ml
UA3	Cumulative As(III) quantity in urine	μmol As
UA5	Cumulative As(V) quantity in urine	μmol As
UDMA	Cumulative MMA quantity in urine	μmol As
UIA	Cumulative As inorganic quantity in urine	μmol As
UMMA	Cumulative DMA quantity in urine	μmol As
UTOT	Cumulative total As quantity in urine	μmol As
V_{alv}	Total volume of alveoli in the lung	cm^3
V_{gen}	Volume of the airways in a generation	cm^3
V_m	Michaelis–Menten maximum rate constant	μmol/hr
$V_{m_{DMA}}$	Second methylation Michaelis–Menten maximum rate constant	μmol/hr
$V_{m_{MMA}}$	First methylation Michaelis–Menten maximum rate constant	μmol/hr
Y	Physiological variable	g
α	Weibel fraction of airway surface alveolated	cm^2
Δt	Time for an aerosol front to pass through a given generation	sec
DF	Rate of change in F of total alveolar volume in generation (z)	
dz		
ρ	Density	g/cm^3
μ	Arithmetic mean of the logtransformed distribution	—
η	Dynamic viscosity of air	cm/sec
Subscripts		
i	Tissue	
in	Inertial impaction	
int	Interstitial	
j	As compound	
x	Lung compartment: NP, TB, or R	
z	''Model A'' Weibel lung generation	

Mathematical Equations

This section describes the mathematical equations used in the model for arsenic deposition and clearance in the lungs and the GI tract. The mathematical equations for the distribution between the different tissues and the excretions were described in a previous paper (Mann *et al.*, 1996).

Lungs. The dust fraction that penetrates the respiratory system is calculated with the harmonized equations (ISO, 1992; Soderholm, 1989). The fractions of the ambient air concentration of airborne particles that penetrate the three lung compartments are defined by the following: SI for inhalable dust fraction, ST for the thoracic dust fraction, and SR for the respirable dust fraction.

The deposition of the penetrated dust in the nasopharynx (SNP(Dae)) is a function of the aerodynamic diameter (Dae), the tidal volume (TV), and the breathing frequency (BF) (James *et al.*, 1989):

$$\mathrm{SNP(Dae)} = 1 - \frac{1}{1.5 \times 10^{-5} \cdot (\mathrm{Dae}^2 \cdot (\mathrm{TV} \cdot \mathrm{BF})^{2/3} \cdot \mathrm{TV}^{1/4})^{1.7} + 1}. \quad (1)$$

The deposition of the penetrated dust into the TB and P compartments was calculated with the equations of Taulbee and Yu (1975) and Weibel (1963). The lung Model A of Weibel consists of 23 generations. The deposition was calculated for each generation for a given diameter. Then, for each diameter, the total deposition, the deposition in the tracheobronchial compartment (STB(Dae)) for generations 1 to 16, and the deposition in the alveolar region (SPP(Dae)) for generations 17 to 23 were calculated.

The following are the calculations of the deposition for each generation (z):

$$S(\text{Dae}) = S_{\text{in(lung)}} + S_{\text{s}} + S_{\text{s,alv}} + S_{\text{d}} + S_{\text{d,alv}} \quad (\text{sec}^{-1}) \tag{2}$$

$$S_{\text{s}} = (1 - \alpha) \cdot \frac{1 - \exp\left[- \frac{2g\tau\Delta t}{\sqrt{\pi A}} \right]}{\Delta t} \quad (\text{sec}^{-1}) \tag{3}$$

$$S_{\text{d}} = (1 - \alpha) \cdot \frac{1 - \exp\left[- \frac{36 D_{\text{B}} \Delta t}{\sqrt{\pi A}} \right]}{\Delta t} \quad (\text{sec}^{-1}) \tag{4}$$

$$S_{\text{s,alv}} = \frac{1.13\ g\tau N_{\text{alv}}^{1/3} V_{\text{alv}}^{2/3} \frac{dF}{dz}}{V_{\text{gen}} + \hat{a}} \quad (\text{sec}^{-1}) \tag{5}$$

$$S_{\text{d,alv}} = \frac{4.23\ N_{\text{d,alv}}^{1/3} V_{\text{alv}}^{2/3} \frac{dF}{dz} \left(\frac{D_{\text{B}}}{\pi \Delta t} \right)^{1/2}}{V_{\text{gen}} + \hat{a}} \quad (\text{sec}^{-1}) \tag{6}$$

$$S_{\text{in(lung)}} = \frac{2\theta_{\text{b}}}{\pi \Delta t} St \left(1 + \frac{\pi}{2R_{\text{c}}} + \frac{2}{3R_{\text{c}}^2} \right), \quad (\text{sec}^{-1}), \tag{7}$$

where

$$\tau = \frac{\text{Dae}^2 (r_{\text{particle}} - r_{\text{air}})}{18 \text{ hr}}$$

$$D_{\text{B}} = \frac{kT}{3\pi\eta \text{Dae}}.$$

With Eq. (2), the deposition for one aerodynamic diameter [SG_z(Dae)] in generation z can be calculated as

$$\text{SG}_z(\text{Dae}) = 1 - \exp[-S(\text{Dae}) \cdot \Delta t]. \tag{8}$$

With Eq. (8) giving the deposition in generation z, the deposition in the tracheobronchial compartment for one aerodynamic diameter STB(Dae) can be calculated, assuming that the TB compartment consists of generations 1–16:

$$\text{STB(Dae)} = \sum_{z=1}^{16} \text{SG}_z(\text{Dae}). \tag{9}$$

With Eq. (8) giving the deposition in generation z, the deposition in the pulmonary compartment for one aerodynamic diameter SPP(Dae) can be calculated, assuming that the pulmonary compartment consists of generations 17–23:

$$\text{SPP(Dae)} = \sum_{z=17}^{23} \text{SG}_z(\text{Dae}). \tag{10}$$

The deposition fraction from the airborne concentration for a given aerodynamic diameter D_x(Dae), where x stands for the three pulmonary compartments (NP, TB, and P), is calculated as follows:

$$D_{\text{NP}}(\text{Dae}) = \text{SI(Dae)} \cdot \text{SNP(Dae)} \tag{11}$$

$$D_{\text{TB}}(\text{Dae}) = \text{ST(Dae)} \cdot \text{STB(Dae)} \tag{12}$$

$$D_{\text{P}}(\text{Dae}) = \text{SR(Dae)} \cdot \text{SPP(Dae)}. \tag{13}$$

The fraction of the airborne particles deposited in the three compartments for a given interval (FD_x(dDae)) is calculated as follows:

$$\text{FD}_x(\text{dDae}) = \frac{D_x(\text{Dae}) + D_x(\text{Dae} + \text{dDae})}{2} \cdot \text{fraction of particles (dDae)}. \tag{14}$$

Finally, the rate of deposition of dust in the three lung compartments is dependent on the breathing frequency (BF), the tidal volume (TV), the air concentration (CONC), and the sum of the percentage of dust deposited:

$$\text{Rate of deposition}_x = \text{BF} \cdot \text{TV} \cdot \text{CONC} \cdot \sum_{0.1}^{\text{Dae}} \%\ D(\text{dDae})_x \quad (\mu\text{g/hr}). \tag{15}$$

The rate constants for absorption from the lung compartments to the plasma depend on the surface area of the compartments. The areas of the three lung compartments are scaled to body weight according to Eqs. (16), (17), and (18). The lung absorption rate is expressed as a quantity of arsenic absorbed per surface area of lung and time (k_{abslung}) and the same rate is applied to the three compartments (Eq. (19)).

Lung_i area:

$$\text{Nasopharynx area} = 2.371 \cdot \text{BW} + 11.007 \quad (\text{cm}^2) \tag{16}$$

$$\text{Tracheobronchial area} = 71.662 \cdot \text{BW} + 19.685 \quad (\text{cm}^2) \tag{17}$$

$$\text{Pulmonary area} = 9917.92 \cdot \text{BW} + 18{,}216.87 \quad (\text{cm}^2) \tag{18}$$

$$dq_{\text{lung}i,j}/dt = \cdots - k_{\text{abslung}} \cdot q_{\text{lung}i,j} \cdot \text{lung}_i \text{ area}, \tag{19}$$

where $q_{\text{lung}i,j}$ is the quantity in lung compartment i (μmol), lung_i area is the lung compartment i area (cm^2), and k_{abslung} is the lung absorption rate constant (liters/$\text{cm}^2 \cdot$ hr).

GI tract. For a better physiological description of the GI tract in the PB-PK model, absorption in the liver and

excretion in the feces are expressed by taking into account the stomach volume (Eq. (20)). The stomach lumen volume (V_{stomach}) and the feces excretion rate (k_{el}) are scaled to body weight. This has the advantage of taking into account the differences between the animal species. The previous PB-PK model used an absorption rate constant taking into account only the quantity of arsenic in the GI tract and used the same excretion rate for all animal species, which is not accurate.

$$dq_{\text{GI tract}\cdot j}/dt = \cdots - k_{\text{el}} \cdot (q_{\text{GI tract}\cdot j}/V_{\text{stomach}}) - k_{\text{abs}} \cdot (q_{\text{GI tract}\cdot j}/V_{\text{stomach}}). \quad (20)$$

The scaling of V_{stomach} used in the PB-PK model is given by

$$V_{\text{stomach}} = 4.5241 \cdot \text{BW}^{0.966} \quad \text{(ml)}. \quad (21)$$

and was obtained by the data in the literature for mammals. The feces excretion rate represents the movement of the lumen in the small intestine (sint) and is calculated as the speed of the fluid times the section of the small intestine (Eq. (24)). The speed in the small intestine is scaled according to Ruckebusch *et al.* (1981), who proposed a speed scaled to the length of the small intestine for mammals (Eq. (23)). The other parameters of the GI tract are scaled according to values taken from the literature for mammals.

$$k_{\text{el}} = \text{rate}_{\text{sint}} \cdot \text{section}_{\text{sint}} \quad \text{(ml/hr)} \quad (22)$$

$$\text{Rate}_{\text{sint}} = 0.79 \cdot \text{length}_{\text{sint}} + 3.95 \quad \text{(cm/min)} \quad (23)$$

$$\text{Section}_{\text{sint}} = \text{volume}_{\text{sint}}/\text{length}_{\text{sint}} \quad (\text{cm}^2) \quad (24)$$

$$\text{Length}_{\text{sint}} = 119.4 \cdot \text{BW}^{0.328} \quad \text{(cm)} \quad (25)$$

$$\text{Volume}_{\text{sint}} = 5.878 \cdot \text{BW}^{0.989} \quad (\text{cm}^3) \quad (26)$$

$$k_{\text{el}} = (56.60 \cdot \text{BW}^{0.328} + 237) \cdot 0.0492 \cdot \text{BW}^{0.661} \quad \text{(ml/hr)}. \quad (27)$$

ACKNOWLEDGMENT

This work was supported by Grant RP 3370-02 from the Electric Power Research Institute, Palo Alto, California.

REFERENCES

American Conference of Governmental Industrial Hygienists (ACGIH) (1993). *Threshold Limit Values of Chemical Substance and Physical Agents and Biological Exposure Indices,* pp. 44. ACGIH. Cincinnati, OH.

Andersen, W. E. (1991). Physiological modelling of organic compounds. *Ann. Occup. Hyg.* **35,** 309–321.

Berner, B., and Cooper, E. R. (1985). Models of skin permeability. In *Transdermal Delivery of Drugs* (A. F. Kydonieu and B. Berner, Eds.), Vol. II, pp. 41–55. CPR Press, Boca Raton, FL.

Buchet, J. P., Lauwerys, R., and Roels, H. (1981a). Comparison of the urinary excretion of arsenic metabolites after a single oral dose of sodium arsenite, monomethylarsonate, or dimethylarsinate in man. *Int. Arch. Occup. Environ. Health* **48,** 71–79.

Buchet, J. P., Lauwerys, R., and Roels, H. (1981b). Urinary excretion of inorganic arsenic and its metabolites after repeated ingestion of sodium metaarsenite by volunteers. *Int. Arch. Occup. Environ. Health* **48,** 111–118.

Droz, P. O. (1978). Contribution à la recherche d'indices biologiques d'exposition aux solvants: Détermination de leurs coefficients de partage et étude de leur comportements dans l'organisme à l'aide de modèles de simulation. Thesis, Neuchâtel University, Switzerland.

Droz, P. O. (1986). Simulation models for organic solvents. In *Safety and Health Aspects of Organic Solvents,* pp. 73–87. A. R. Liss, New York.

Fiserova-Bergerova, V., and Hughes, H. C. (1983). Species differences on bioavailability of inhaled vapors and gases. In *Modeling of Inhalation Exposure to Vapors: Uptake, Distribution, and Elimination* (V. Fiserova-Bergerova, Ed.), Vol. II, pp. 97–106. CRC Press, Boca Raton, FL.

Ginsburg, J. M. (1965). Renal mechanism for excretion and transformation of arsenic in the dog. *Am. J. Physiol.* **208,** 832–840.

Hopenhayn-Rich, C., Smith, A. H., and Goeden, H. M. (1993). Human studies do not support the methylation threshold hypothesis for the toxicity of inorganic arsenic. *Environ. Res.* **60,** 161–177.

Hughes, M. F., Menache, M., and Thompson, D. J. (1994). Dose-dependent disposition of sodium arsenate in mice following acute oral exposure. *Fundam. Appl. Toxicol.* **22,** 80–89.

International Commission on Radiological Protection (ICPR) (1992). *Report of the Task Group on Reference Man,* ICPR Publication No. 23, 5th ed. Pergamon, Elmsford, NY.

International Organization for Standardization (ISO) (1991). Air quality—Particle size fraction definitions for health-related sampling. Approved for publication as CD 7708, Geneva.

International Organization for Standardization (ISO) (1992). Standard CD7708. Particle size fraction definition for health sampling. ISO, Geneva.

James, A. C., Birchall, A., Cross, F. T., Cuddihy, R. G., and Johnson, J. R. (1989). The current approach of the ICPR task group for modeling doses to respiratory tract tissues. *Health Phys.* **57,** 171–282.

Johnson, J. R., and Milencoff, S. (1989). A comparison of excretion and retention between the surrent ICPR lungs model and proposed new model. *Health Phys.* **57,** 263–270.

Lindstedt, S. L. (1992). Allometric extrapolation. In *International Workshop on Physiologically Based Pharmacokinetic Modeling and Risk Assessment,* August 3–21, Fort Collins, CO.

Mann, S., Droz, P. O., Diezi, J., Meister, S., and Nenninger, M. (1995). Preliminary results of in vitro measurements of the affinities of arsenic metabolites for several tissues in hamsters. SEGH, Second International Conference on Arsenic Exposure and Health Effects, June 12–14, San Diego, CA.

Mann, S., Droz, P. O., and Vahter, M. (1996). A physiologically based pharmakokinetic model for arsenic exposure. I. Development in hamsters and rabbits. *Toxicol. Appl. Pharmacol.* **137,** 8–22.

Offergelt, J. A., Roels, H., Buchet, J. P., Boeckx, M., and Lauwerys, R. (1992). Relationship between airborne arsenic trioxide and urinary excretion of inorganic arsenic and its methylated metabolites. *Br. J. Ind. Med.* **49,** 387–393.

Persons, D. D., Hess, G. G., Muller, W. J., and Scherer, (1987). Airway

deposition of hygroscopic heterodispersed aerosols: results of a computer calculation. *J. Appl. Physiol.* **63,** 1195–1204.

Ruckebusch, Y., Bueno, L., and Fioramonti, J. (1981). L'intestin grele. In *La Mécanique Digestive Chez les Mamifères,* Chap. 5, p. 78. Masson, Paris.

Soderholm, S. C. (1989). Proposed international conventions for particles size-selective sampling. *Ann. Occup. Hyg.* **33,** 301–320.

Tam, G. K. H., Charbonneau, S. M., and Bryce, F. (1979). Metabolism of inorganic arsenic (74As) in humans following oral ingestion. *Toxicol. Appl. Pharmacol.* **50,** 319–322.

Taulbee, D. B., and Yu, C. P. (1975). A theory of aerosol deposition in the human respiratory tract. *J. Appl. Physiol.* **38,** 77–85.

Vahter, M. (1981). Biotransformation of trivalent and pentavalent inorganic arsenic in mice and rats. *Environ. Res.* **25,** 286–293.

Vahter, M. (1989). Arsenic. Environmental and occupational exposure to arsenic. In *Assessment of Inhalation Hazards* (U. Mohr, Ed.), ILSI monographs. Springer-Verlag, Berlin.

Vahter, M., Friberg, L., Rahnster, B., Nygern, A., and Nolinder, P. (1986). Airborne arsenic and urinary excretion of metabolites of inorganic arsenic among smelter workers. *Int. Arch. Occup. Environ. Health* **57,** 79–91.

Weibel, E. R. (1963). *Morphology of the Human Lung.* Springer-Verlag, New York.

World Health Organization (WHO) (1993). *Guidelines for Drinking-Water Quality,* 2nd ed., Vol. 1, pp. 176. WHO, Paris, France.